

**Unifying autocatalytic and zeroth order
branching models for growing actin networks
– Supporting Information –**

Julian Weichsel,^{1,2,*} Krzysztof Baczynski,¹ and Ulrich S. Schwarz^{1,†}

¹*Bioquant and Institute for Theoretical Physics, University of Heidelberg, Germany*

²*Department of Chemistry, University of California at Berkeley, United States*

I. LINEAR STABILITY ANALYSIS OF THE SIMPLIFIED MODEL EQUATIONS

To analyze analytically the fixed points of Eq. (4) of the main text, we simplify the equation by integrating over angle bins of size $\Delta\theta = 35^\circ$ (i.e. half the assumed Arp2/3 branching angle) and neglecting filaments growing in directions $|\theta| > 87.5^\circ$. Branching is assumed to be restricted to pairs of angle bins with a relative angle difference of 70° . This yields the coupled equations

$$\begin{aligned}\partial_t N_{0^\circ} &= \frac{1}{2} k_b \frac{N_{\pm 70^\circ}}{\left(\sum_i N_i\right)^{1-\mu}} - k_c N_{0^\circ} \\ \partial_t N_{\pm 35^\circ} &= \frac{1}{2} k_b \frac{N_{\pm 35^\circ}}{\left(\sum_i N_i\right)^{1-\mu}} - (k_c + k_{\text{gr}}^{35^\circ}) N_{\pm 35^\circ} \\ \partial_t N_{\pm 70^\circ} &= k_b \frac{N_{0^\circ}}{\left(\sum_i N_i\right)^{1-\mu}} - (k_c + k_{\text{gr}}^{70^\circ}) N_{\pm 70^\circ}.\end{aligned}\tag{S1}$$

The two physically meaningful steady states of this system are given as Eq. (5) and Eq. (6) of the main text. Analyzing the eigenvalues of the Jacobian matrix reveals that neither fixed point is stable for $\mu > 1$. For $\mu \leq 1$, all but one eigenvalue are attracting, while the remaining one changes sign in the relevant parameter range in each case and yields mutually exclusive stability of the two possible fixed points. For $\mu \leq 1$, stability switches when the simple condition

$$k_{\text{gr}}^{70^\circ} = -k_c + 4k_{\text{gr}}^{35^\circ} + \frac{2(k_{\text{gr}}^{35^\circ})^2}{k_c}\tag{S2}$$

is fulfilled. Remarkably, this stability criterion does not depend on the specific branching rate parameter k_b nor on the reaction order parameter μ . Rather, it turns out that for $\mu < 1$ any combination of k_b and μ only scales the total number of filaments in steady state as

*Electronic address: weichsel@berkeley.edu

†Electronic address: ulrich.schwarz@bioquant.uni-heidelberg.de

$(k_b/\sqrt{2k_c(k_c + k_{gr}^{70^\circ})})^{1/(1-\mu)}$ for the +70/0/-70 pattern and as $(k_b/(2(k_c + k_{gr}^{35^\circ})))^{1/(1-\mu)}$ for the ± 35 pattern (cf. Eq. (5)–Eq. (7) of the main text). This scaling of *total* filament number however, does not have any impact whatsoever on the *relative* filament number present in different angle bins and thus on the stability of a particular orientation pattern in steady state. Furthermore, also for $\mu = 1$ the stability condition of the fixed points Eq. (S2) remains unchanged, but for each of the two fixed points to yield finite filament densities, an additional constraint has to be satisfied as is discussed in detail in the main text. This constraint in both cases relates k_b to a combination of the capping rate k_c and via the outgrowth rate k_{gr}^θ to the network velocity v_{nw} . Additionally, Eqs. (S1) become linear and thus the absolute filament number in steady state is not determined by the given set of parameters anymore, but rather by an arbitrary initial condition, as is expected for autocatalytic growth.

II. MAPPING OF THE ARP2/3 ACTIVATION MODEL TO THE BRANCHING RATE PARAMETERS k_b AND μ IN THE ACTIN GROWTH MODEL

The equation for actin network dynamics (Eq. (4) of the main text) and its subsequent stability analysis yields the network pattern that is realized in steady state for a given combination of the model parameters, which are network velocity v_{nw} , capping rate k_c , branching rate k_b and reaction order μ . As explained above, the stability criterion Eq. (S2) for the two different patterns does not depend on the precise value of the branching rate k_b and the order of the branching reaction μ as long as $k_b > 0$ and $\mu \leq 1$.

Our unifying model is obtained by coupling the Arp2/3 activation model Eq. (1) with a variable branching rate $k_b(N_{fil}) = B^{ss}(N_{fil})$ to the actin growth model Eq. (4) with $\mu = 0$. The number of filaments in the Arp2/3 activation model is obtained from the actin growth model as $N_{fil} = \int N(\theta) d\theta$. B^{ss} corresponds to the branching term of Eq. (1) in steady state, i.e. $B^{ss}(N_{fil}) = \tilde{k}_b A_{ss} P_{ss}$ as plotted in Fig. 2 of the main text. Upon changing the network velocity v_{nw} , this procedure yields a sequence of stable fixed points as shown in Fig. 4 of the main text.

We now show that the two modelling approaches (actin growth model with constant reaction order $0 \leq \mu \leq 1$ and unifying model combining Arp2/3 activation model and actin growth model) are equivalent in the sense that within the linear regime around any fixed point of our models, the effective branching rate B^{ss} can be written as $B^{ss} = k_b N_{fil}^\mu$, such that reaction order μ and branching rate k_b are locally constant and satisfy the stability condition of the fixed point (i.e. $k_b > 0$ and $\mu \leq 1$).

Consider a small neighborhood around an arbitrary fixed point at filament density $N_{\text{fil}0}$, in which we can write the effective branching rate of the Arp2/3 reaction model B^{ss} as a first order expansion,

$$B^{\text{ss}}(N_{\text{fil}}) = \tilde{k}_{\text{b}} A_{\text{ss}} P_{\text{ss}} \simeq \hat{a}(N_{\text{fil}0}) + \hat{b}(N_{\text{fil}0})(N_{\text{fil}} - N_{\text{fil}0}) = a(N_{\text{fil}0}) + b(N_{\text{fil}0})N_{\text{fil}}, \quad (\text{S3})$$

where $\hat{a}(N_{\text{fil}0})$ and $\hat{b}(N_{\text{fil}0})$ are the corresponding coefficients of the expansion of $B^{\text{ss}}(N_{\text{fil}})$ around $N_{\text{fil}0}$. Similarly, we expand the branching term of the actin growth model, $k_{\text{b}}N_{\text{fil}}^{\mu}$ (cf. Eq. (S1) and Eq. (4)), around $N_{\text{fil}0}$,

$$k_{\text{b}}N_{\text{fil}}^{\mu} \simeq k_{\text{b}}N_{\text{fil}0}^{\mu} + k_{\text{b}}\mu N_{\text{fil}0}^{\mu-1}(N_{\text{fil}} - N_{\text{fil}0}) = (1 - \mu)k_{\text{b}}N_{\text{fil}0}^{\mu} + k_{\text{b}}\mu N_{\text{fil}0}^{\mu-1}N_{\text{fil}}. \quad (\text{S4})$$

Mapping the coefficients of Eq. (S3) and Eq. (S4) yields relations for the parameters k_{b} and μ , which are constant within the linear regime around $N_{\text{fil}0}$:

$$\begin{aligned} a(N_{\text{fil}0}) &= (1 - \mu)k_{\text{b}}N_{\text{fil}0}^{\mu} \\ b(N_{\text{fil}0}) &= k_{\text{b}}\mu N_{\text{fil}0}^{\mu-1}. \end{aligned} \quad (\text{S5})$$

To ensure consistency with our linear stability analysis, we further need to show, that based on Eq. (S5) the two parameters exclusively occupy the stable regime $k_{\text{b}} > 0$ and $\mu \leq 1$. Then the fixed points obtained by the stability analysis in the previous section and in the main text are stable at their corresponding (self-consistent) values of k_{b} and μ as determined by the Arp2/3 activation model. In the following, for illustration we will discuss the low and high filament density cases as examples and subsequently generalize to the case of arbitrary $N_{\text{fil}0}$.

First, consider $N_{\text{fil}0} \ll N_{\text{trans}}$, where N_{trans} indicates some intermediate filament number in between the first and zeroth order regime as illustrated in Fig. 2. Here, $N_{\text{fil}0}$ corresponds to a fixed point at sufficiently low filament number, such that autocatalytic branching dominates and the effective branching is proportional to the number of filaments, $B^{\text{ss}} = k_{\text{b}}^{\text{ac}}N_{\text{fil}}$ (cf. Eq. (2) of the main text). Therefore, $a(N_{\text{fil}0}) = 0$ and $b(N_{\text{fil}0}) = k_{\text{b}}^{\text{ac}}$ holds, and we obtain from Eq. (S5),

$$k_{\text{b}} = k_{\text{b}}^{\text{ac}} \quad \text{and} \quad \mu = 1. \quad (\text{S6})$$

Similarly for $N_{\text{fil}0} \gg N_{\text{trans}}$, we obtain $a(N_{\text{fil}0}) = B_{\infty}^{\text{ss}}$ and $b(N_{\text{fil}0}) = 0$ (cf. Eq. (3) of the main text) and therefore,

$$k_{\text{b}} = B_{\infty}^{\text{ss}} \quad \text{and} \quad \mu = 0, \quad (\text{S7})$$

as expected.

Now consider the case of $N_{\text{fil}0} \sim N_{\text{trans}}$, at arbitrary filament number somewhere in between the first and zeroth order regimes. From the analysis of the Arp2/3 reaction model in the main text, we already know that, within the physically relevant parameter regime, the branching term is determined by the steady state of Eq. (1) as $B^{\text{ss}}(N_{\text{fil}}) = \tilde{k}_b A_{\text{ss}} P_{\text{ss}}$ and will prototypically look like the specific example shown in Fig. 2. In general, at low filament density the function exhibits a linear regime, which levels off as filament density increases and finally approaches a constant regime. Therefore, $a(N_{\text{fil}0})$ and $b(N_{\text{fil}0})$ are nonnegative, continuous and monotonic functions of $N_{\text{fil}0}$, varying within the boundaries,

$$\begin{aligned} 0 &\leq a(N_{\text{fil}0}) \leq B_{\infty}^{\text{ss}} \\ k_b^{\text{ac}} &\geq b(N_{\text{fil}0}) \geq 0, \end{aligned} \tag{S8}$$

as $N_{\text{fil}0}$ increases from $N_{\text{fil}0} \ll N_{\text{trans}}$ through $N_{\text{fil}0} \sim N_{\text{trans}}$ to $N_{\text{fil}0} \gg N_{\text{trans}}$. For increasing filament number, beginning from $N_{\text{fil}0} \ll N_{\text{trans}}$, $a(N_{\text{fil}0})$ increases from 0, while $b(N_{\text{fil}0})$ decreases from k_b^{ac} until at $N_{\text{fil}0} \gg N_{\text{trans}}$, $a(N_{\text{fil}0})$ approaches B_{∞}^{ss} , and $b(N_{\text{fil}0})$ continuously goes to 0. It is therefore always possible to find a combination, $k_b > 0$ and $\mu \leq 1$, that fulfills Eq. (S5), is constant within the linear regime around $N_{\text{fil}0}$, and thus yields a stable fixed point within the calculated phase diagram as predicted from linear stability analysis (i.e. Fig. 3 of the main text).

In Fig. S1, the resulting parameter combinations k_b and μ as well as a and b (inset) are calculated as functions of $N_{\text{fil}0}$ using the first order expansion of $B^{\text{ss}}(N_{\text{fil}}) = \tilde{k}_b A_{\text{ss}} P_{\text{ss}}$ in combination with Eq. (S5) for the same parameters as used in Fig. 2 of the main text. It is evident, that the order of the branching reaction changes continuously from first to zeroth order as the steady state number of filaments increases.

III. EXPERIMENTAL VALUES FOR THE MODEL PARAMETERS

In the following we will relate, where possible, our model parameters to quantitative values that have been experimentally measured before. As the precise activation cascade of the Arp2/3 complex is still unknown and a subject of current research, the generic Arp2/3 activation model used here merely reflects a possible and realistic scenario which interpolates between the two extreme cases of first and zeroth order branching. Consequently not all model parameters that enter the equations have been experimentally accessible so far. However, as is discussed in the main text, our key assumption that the limiting factor in growing actin networks at sufficiently high filament density is the available amount of activated Arp2/3 is very plausible indeed [1]. As long as this is the case, the specific details of the Arp2/3 activation cascade are expected to only have a minor

impact on our results and do not change the key characteristics resulting from our analysis.

In steady state, the model parameter network velocity v_{nw} is bounded between zero and the free barbed end polymerization speed of a single actin filament at v_{fil} and can be adjusted experimentally for instance by applying an opposing load against the growing network. The barbed end polymerization speed is determined by the (de-)polymerization kinetics of single filament barbed ends (with on and off rates, $k_{\text{fil}}^+ = 11.6 \mu\text{M}^{-1}\text{s}^{-1}$ and $k_{\text{fil}}^- = 1.4 \text{s}^{-1}$ [2]), the concentration of globular actin in solution ($c_{\text{actin}} \simeq 7 \mu\text{M}$ has been used in typical in-vitro assays [3, 4]) and the individual growth increment of actin polymerization, $\delta_{\text{fil}} \simeq 2.7 \text{nm}$ [5]: $v_{\text{fil}} = (k_{\text{fil}}^+ c_{\text{actin}} - k_{\text{fil}}^-) \delta_{\text{fil}} \sim 200 \text{nm/s}$; The concentration of obstacle bound nucleation promoting factors P_0 can be adjusted in experiment, for instance within $0.01 \text{nm}^{-2} \leq P_0 \leq 0.15 \text{nm}^{-2}$ in case of N-WASP on plastic beads [3].

The rate parameters in the actin growth model are the branching rate k_b and the order of the branching reaction μ , the capping rate k_c , and filament outgrowth from the reaction zone where branching is possible with rate k_{gr}^θ . A combination of k_b and μ is determined in steady state by the Arp2/3 activation model as discussed above. Therefore, specific values for the branching rate constant have to be associated with the relevant regime. It has been estimated before that $k_b \equiv k_b^{\text{ac}} \sim 0.43 \text{s}^{-1}$ per filament within the first order (autocatalytic) branching regime ($\mu = 1$) [6], while in the zeroth order regime ($\mu = 0$), $k_b \equiv P_0 k_{\text{act}} \sim 10 \text{s}^{-1}$ has been assumed to be active in the tail of propelled plastic beads in-vitro [7]. Capping rates have been measured in the range $k_c = 2.3 - 6.5 \mu\text{M}^{-1}\text{s}^{-1}$ [8] and typical in-vitro capping protein concentrations are around $0.1 \mu\text{M}$ [3, 4]. Outgrowth in the model is determined by the filament growth velocity v_{fil} relative to the network speed v_{nw} as well as the width of the branching region d_{br} , in which interaction of filaments with Arp2/3, activation by NPFs and branching is possible,

$$k_{\text{gr}}^\theta(v_{\text{nw}}) = \begin{cases} 0 & \text{if } |\theta| \leq \arccos(v_{\text{nw}}/v_{\text{fil}}) \\ \frac{v_{\text{nw}} - v_{\text{fil}} \cos \theta}{d_{\text{br}}} & \text{if } |\theta| > \arccos(v_{\text{nw}}/v_{\text{fil}}) \end{cases}. \quad (\text{S9})$$

Here d_{br} is a length scale in the nanometer range. Hence, where applicable $d_{\text{br}} = 2\delta_{\text{fil}} = 5.4 \text{nm}$ is used in the model. Thus outgrowth of filaments at a typical angle of $\theta = \pm 70^\circ$ at an intermediate network velocity of $v_{\text{nw}} = v_{\text{fil}}/2$ is expected to occur at around $k_{\text{gr}}^{\pm 70^\circ}(v_{\text{fil}}/2) \sim 6 \text{s}^{-1}$ per filament. Finally, we can estimate the approximate lateral network width relevant in the model by comparing N_{fil} to the number of filaments per leading edge length close to the membrane in migrating cells, which is around $90 \pm 10 \mu\text{m}^{-1}$ [9].

IV. SUPPORTING FIGURES

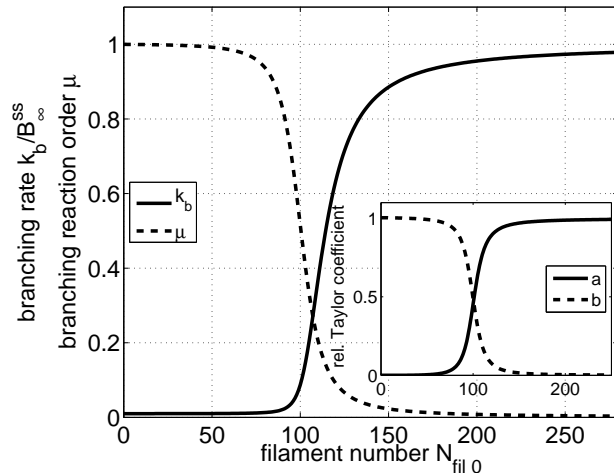


FIG. S1: Dependence of k_b and μ as well as a and b (inset) on the steady state filament number $N_{fil 0}$ as calculated from Eq. (S5) and Eq. (S3) respectively. k_b and μ never leave the stable regime as determined by linear stability analysis above (i.e. $k_b > 0$ and $\mu \leq 1$).

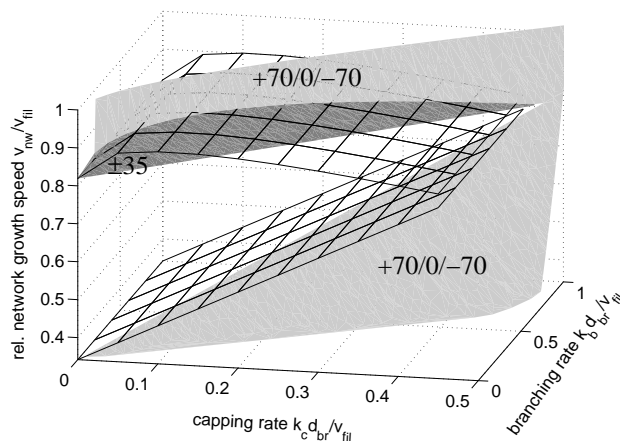


FIG. S2: Phase diagram from stability analysis of the analytical model. The three dimensional parameter space is spanned by the parameters k_c , k_b and v_{nw} . The $+70/0/-70$ pattern is stable above and below the two meshed surfaces, while the ± 35 pattern is stable in between. For $\mu = 1$ (autocatalytic growth) and each combination of k_c and k_b , within the available subspace, only one network growth velocity yields finite filament number in steady state and so the accessible parameter range is restricted to the dark and light gray surfaces for the ± 35 and $+70/0/-70$ patterns, respectively. To better visualize the three dimensionality of the plot, we also provide a movie in which the diagram is rotated in space ([movie.mov](#)).

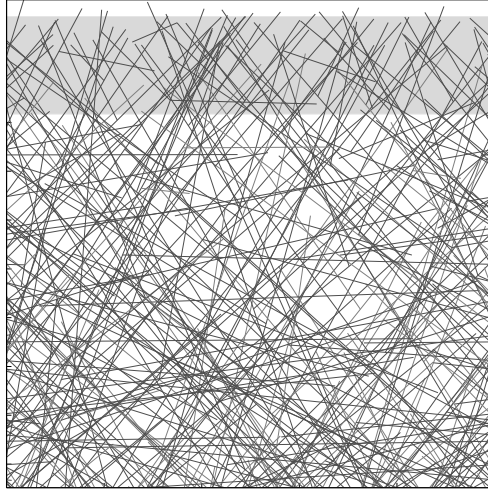


FIG. S3: Representative snapshot of a growing actin network in a stochastic computer simulation. Actin filament growth occurs up to the surface of a rigid obstacle moving towards the top with velocity v_{nw} . Each filament end grows deterministically with the polymerization velocity v_{fil} . Filament ends in the reaction zone of width d_{br} (light gray) are additionally subject to stochastic capping and branching reactions according to a kinetic Monte Carlo procedure. Filaments cross each other without interacting. Horizontally we employ periodic boundary conditions. For more details compare [10].

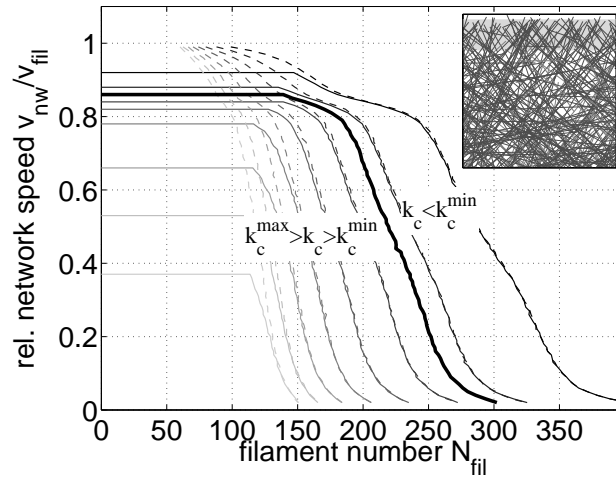


FIG. S4: N_{fil} versus v_{nw} curves obtained from the stochastic computer simulations. A reduced version of this figure is given as inset of Fig. 4 in the main text.

V. SUPPORTING MOVIE

To illustrate the three dimensionality of our phase diagram (Fig. 2 in the main text), we provide a movie in which the three-dimensional diagram is rotated in space ([movie.mov](#)).

-
- [1] T. D. Pollard, L. Blanchoin, and R. D. Mullins. Molecular mechanism controlling actin filament dynamics in nonmuscle cells. *Annual Reviews in Biophysics and Biomolecular Structure*, 29(1):545–576, 2000.
 - [2] T. D. Pollard. Rate constants for the reactions of ATP-and ADP-actin with the ends of actin filaments. *The Journal of Cell Biology*, 103(6):2747–2754, 1986.
 - [3] S. Wiesner, E. Helfer, D. Didry, G. Ducouret, F. Lafuma, M. F. Carlier, and D. Pantaloni. A biomimetic motility assay provides insight into the mechanism of actin-based motility. *Journal of Cell Biology*, 160(3):387–398, 2003.
 - [4] Y. Marcy, J. Prost, M. F. Carlier, and C. Sykes. Forces generated during actin-based propulsion: a direct measurement by micromanipulation. *Proceedings of the National Academy of Sciences of the United States of America*, 101(16):5992–5997, 2004.
 - [5] B. Alberts, A. Johnson, J. Lewis, M. Raff, K. Roberts, and P. Walter. *Molecular Biology of the Cell, Fourth Edition*. Garland, 2002.
 - [6] T. E. Schaus and G. G. Borisy. Performance of a population of independent filaments in lamellipodial protrusion. *Biophysical Journal*, 95(3):1393–1411, 2008.
 - [7] A. Mogilner and G. Oster. Force generation by actin polymerization II: the elastic ratchet and tethered filaments. *Biophysical Journal*, 84(3):1591–1605, 2003.
 - [8] D. A. Schafer, P. B. Jennings, and J. A. Cooper. Dynamics of capping protein and actin assembly in vitro: uncapping barbed ends by polyphosphoinositides. *The Journal of Cell Biology*, 135(1):169–179, 1996.
 - [9] S. A. Koestler, S. Auinger, M. Vinzenz, K. Rottner, and J. V. Small. Differentially oriented populations of actin filaments generated in lamellipodia collaborate in pushing and pausing at the cell front. *Nature Cell Biology*, 10(3):306–313, 2008.
 - [10] J. Weichsel and U. S. Schwarz. Two competing orientation patterns explain experimentally observed anomalies in growing actin networks. *Proc. Natl. Acad. Sci. USA*, 107:6304–9, 2010.